Location of deuterium on the silicon (100) monohydride surface determined by transmission-ion channeling

W. R. Wampler
Sandia National Laboratories, Albuquerque, New Mexico 87185-1056
(Received 15 September 1994)

The location of deuterium (D) in the monohydride configuration on the silicon (100) surface is established using transmission-ion channeling. A 2-MeV $^4He^+$ ion beam was used to elastically recoil D from the beam-exit surface of a thin silicon crystal. The yield of recoiled D was measured versus angle about the ⟨100⟩, ⟨110⟩, and ⟨111⟩ axes. The location of the surface D relative to the silicon lattice was determined by comparing the measured yields with computer-channeling simulations. The observed location is consistent with a Si-D bond length of 1.6 ± 0.2 Å along the silicon tetrahedral bond direction in agreement with recent *ab initio* theoretical calculations.

I. INTRODUCTION

Hydrogen termination of dangling bonds on silicon surfaces can produce beneficial effects for device fabrication. The hydrogen protects the surface from chemical contamination and it reduces carrier recombination at the surface which can improve performance of devices such as solar cells and photodiodes. In addition, surface hydrogen may strongly affect chemical vapor deposition and molecular-beam epitaxial growth processing. These effects may be more clearly understood if the atomic configuration of the hydrogen on the surface is known. Several *ab initio* theoretical calculations have been reported which predict the configuration of hydrogen bound to the Si(100) surface.[1-6] These calculations are generally in good agreement with each other, but there is little experimental data available with which to compare. Although some of the structural features, in particular the (2×1) reconstruction of the Si(100) monohydride, have been elucidated by scanning tunneling microscopy (STM) (Refs. 7 and 8) and low-energy electron diffraction (LEED),[9,10] these techniques do not give the hydrogen location. One recent experimental study,[11] based on low-energy ion scattering, reported a configuration for the Si(100) monohydride surface which differs significantly from the *ab initio* calculations.

Here we use transmission-ion channeling to determine the position of deuterium on a Si(100) monohydride surface. Although the location of surface hydrogen can be determined fairly directly from transmission channeling measurements, use of this technique has been limited mainly by the difficulty of preparing the necessary thin single-crystal samples. Here we describe a method of fabricating thin single-crystal silicon samples. In Sec. II the basic principles behind transmission channeling experiments are discussed, and the equipment and methods used to prepare samples and make the measurements are described. In Sec. III results from axial channeling measurements about the ⟨100⟩, ⟨110⟩, and ⟨111⟩ axes are presented. In Sec. IV the hydrogen location relative to the Si lattice is determined by comparing the channeling data with computer simulations of channeling. This result is then compared with the location predicted by *ab initio* calculations.

II. EXPERIMENTAL METHOD

A. Transmission-ion channeling

Ion channeling has been extensively used to study the location of foreign atoms within a host crystal lattice.[12] The basic principle is illustrated in Fig. 1. When an analysis beam of energetic ions is directed onto a crystal along a high-symmetry direction, Coulomb repulsion deflects the ions away from the rows or planes of lattice atoms toward the center of the open channels. After passing a short distance (~100 nm) through the lattice, an equilibrium distribution of ion flux within the channels is established which has maxima at the center of the channels and minima along the rows of lattice atoms. The flux distribution within the channel strongly depends on the angle between the incident ion flux and the channel direction, becoming more uniform at larger angles. Collisions involving a small impact parameter between

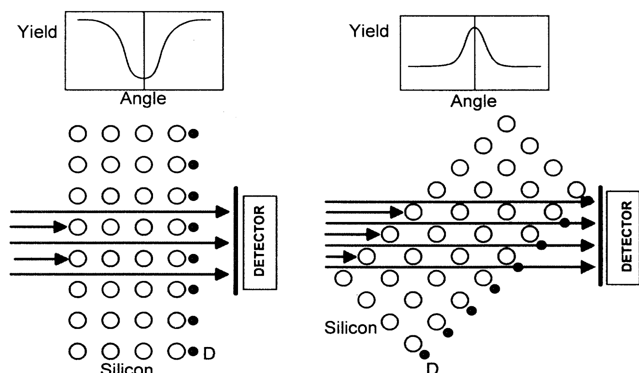

FIG. 1. Schematic illustration of the basic principles of transmission channeling. D on the beam-exit surface in line with rows of Si atoms gives a dip in the channeling yield, whereas D near the center of open channels through the Si lattice gives a peak in the channeling yield.

 ©1995 The American Physical Society

the ions and foreign atoms can be detected by various methods. The yield of such events is proportional to the ion flux at the location of the foreign atom. Typically, one measures the scattering yield from the foreign atom versus angle between the analysis beam and the channeling direction. The location of the foreign atom within the channel can then be determined from the shape of such a channeling scan. For example, if the foreign atom is near the channel center as viewed along the channeling direction, then a peak in the scattering yield will be seen at the channeling direction. Conversely, if the foreign atom is nearly in line with a row of lattice atoms, a dip in the scattering yield will be seen at the channeling direction. Measurements of channeling scans about the major crystallographic directions provide the information needed to determine the position of the foreign atom relative to the host lattice. A computer model can be used to simulate channeling scans for various lattice positions and channel directions, and by comparing the measured scans with the computer simulations the lattice coordinates of the foreign atom can be determined.

If the target crystal is thin enough for the analysis beam to pass through it, the position of foreign atoms on the exit or downstream surface can also be determined by this method. This technique of transmission channeling has previously been used to determine the position of hydrogen on Ni and Pd surfaces,[13–15] and of Ni, Sb, and Ge on Si surfaces.[16,17] Such experiments require a free-standing thin crystal only a few hundred nanometers thick. The flux distribution of the analysis beam within the channels at the exit surface is essentially the same as in the bulk crystal, and is not altered significantly by surface reconstruction. Thus the measured scattering yields depend on the position of the foreign atoms on the surface relative to the bulk crystal lattice in the same way as it would for foreign atoms within the lattice.

B. Sample preparation and characterization

The thin silicon crystals used in this study were prepared from Si(100) wafers with a buried oxide layer. The buried oxide was produced by implanting wafers at 500 °C with 150-keV oxygen ions. The wafers were then annealed, and additional epitaxial silicon was deposited at 1275 °C. This procedure produced a continuous buried layer of SiO_2 0.4 μm thick beneath a single-crystal overlayer 0.4 μm thick. Wafers with buried oxide layers produced by implantation of oxygen (SIMOX) are commercially available. An alternative process of bonding followed by thinning of the top silicon crystal has also been used to produce silicon wafers with a buried oxide layer.[18]

In our studies a SIMOX wafer was diced into samples $9\times9\times0.62$ mm.[3] The substrate was partially removed with a dimple grinder to leave a silicon thickness of about 50 μm at the center of the dimple. The sample was then chemically etched in 4 *M* KOH solution at 80 °C until the substrate was removed over a region about 3 mm in diameter at the center of the dimple. The front surface was protected during grinding and etching of the substrate by bonding the sample with epoxy to a quartz support. The buried SiO_2 layer serves as an etch stop barrier during the KOH etching. Following the KOH etch, the samples were separated from the quartz support by soaking in H_2SO_4:H_2O_2 (2:1). The oxide layer was then removed by etching in buffered oxide etch (BOE), NH_4OH:HF (7:1). The above process yielded thin single crystals of silicon of the high purity and crystalline perfection required for transmission channeling experiments, supported by thicker surrounding substrate material by which samples could be handled during cleaning and mounting.

The procedure described by Ishazaki and Shiraki[19] was used to prepare a clean silicon surface on the thin samples. This consists of alternate rinses in boiling HNO_3, BOE, and deionized water. Final rinses in HCl:H_2O_2:H_2O (3:1:1) followed by deionized water were used to produce a clean thin passivating oxide layer immediately prior to mounting in an UHV chamber. The remainder of the sample preparation and analysis was done with the sample attached to a channeling goniometer in an UHV chamber which had a base pressure of 10^{-10} Torr. Sample mounting was done through a loadlock to maintain UHV conditions in the analysis chamber.

The sample was mounted on a channeling goniometer with three axes of rotation which provided precise angular positioning (within 0.05°) necessary for the channeling measurements. The goniometer also allowed three-dimensional translation of the sample holder for centering the sample on the analysis beam and for translating the sample to various working positions during preparation and characterization of the surface. After mounting the sample in the UHV chamber the sample preparation proceeded as follows. The sample and sample holder were radiatively heated to 400 °C by a tungsten filament located close to the holder. The temperature was measured by a thermocouple attached to the sample holder. The sample temperature was held at 400 °C for 10 min to desorb hydrocarbons. A heat lamp focused on the sample was then turned on for 2 min to raise the sample temperature above 800 °C where the surface oxide desorbs.[19] The sample was quickly cooled back to 400 °C, where it was then exposed to atomic deuterium (D) produced by thermal dissociation of D_2 on a tungsten filament near the sample. The atomic D exposure conditions were chosen to provide a dose sufficient to produce a saturated monohydride-terminated surface. The sample heater was then turned off, allowing the sample to cool to room temperature. All channeling measurements were made with a sample temperature near 25 °C. Contamination of the surface from residual gas in the vacuum system was avoided by minimizing the time between desorbtion of the oxide and formation of the monohydride, both of which greatly reduce the chemical reactivity of the surface.

The composition of the sample surface (excluding D) was examined by Auger electron spectroscopy (AES), and the surface structure was examined by low-energy electron diffraction (LEED). AES showed surface impurities to be below the limit of detection. For carbon and oxygen, the two most likely impurities, the AES detection limit is about 0.05 monolayer. Thermal desorbtion of D

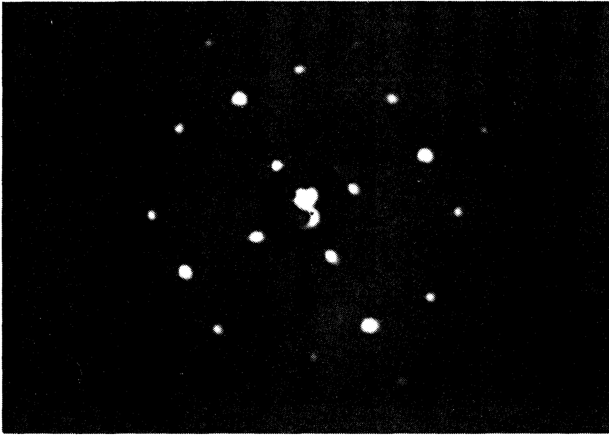

FIG. 2. LEED image showing the 2×1 surface structure taken with an electron energy of 55 eV after dosing the sample with D.

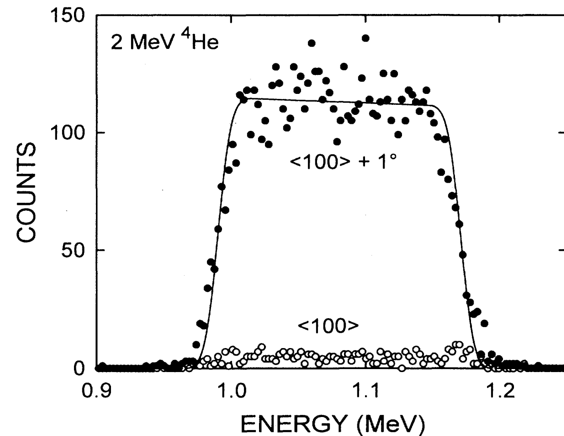

FIG. 3. Backscattering spectrum for 2-MeV ^{4}He from the transmission channeling sample. The open symbols are with the beam aligned with the ⟨100⟩ axis and the filled symbols are with the beam 1° away from the ⟨100⟩ axis. The curve is a computer simulation used to determine the Si thickness.

through inadvertant heating of the sample by the AES electron beam was avoided by keeping the electron-beam current below 1 μA. A sharp (2×1) LEED pattern (shown in Fig. 2) was observed, confirming the dimer surface reconstruction found in previous studies[7–10] for the Si(100) monohydride-terminated surface. Previous STM studies[7] have shown that monohydride Si(100) surfaces prepared as described above have a well-ordered dimerized structure.

Since the thin crystal region must be flat for channeling experiments, its flatness was checked by reflecting a low power HeNe laser beam from the sample. This technique showed that the thin region of the sample was flat within 0.05°. Results from AES, LEED, and laser reflection examinations were the same before and after the channeling measurements, showing that the composition, structure, and flatness of the sample did not change during the channeling measurements.

C. Ion-beam analysis and channeling measurements

The channeling experiments were done by measuring the yield of D elastically scattered from the beam-exit side of the sample. The sample was oriented such that the beam-exit surface was the original top surface of the SIMOX wafer. While exposing the sample to atomic D, the beam-exit side of the sample was facing the atomic D source. However, it was found that the resulting D coverage was close to one monolayer on both the beam-exit and beam-entry sides of the sample. D was therefore removed from the beam-entry surface by sputtering with 500-eV xenon so that yields of scattered D measured during the channeling experiments were only from D on the beam-exit surface.

The analysis beam used for the channeling experiments was $^4He^+$ with an energy near 2 MeV and an angular divergence of 0.03°. The size of the analysis beam spot at the sample was 1×1 mm^2. Two stages of differential pumping along the beamline were used to maintain UHV conditions in the analysis chamber during channeling measurements. Bakeable silicon surface barrier detectors with standard nuclear electronics for pulse-height analysis were used to collect energy spectra of scattered and recoiled particles. One detector for Rutherford backscattering (RBS) faced the beam entry side of the sample, and analyzed ^{4}He backscattered through an angle of 150°. Figure 3 shows a backscattering spectrum taken on a transmission channeling sample with the analysis beam aligned along the ⟨100⟩ axis and a spectrum taken 1° away from the ⟨100⟩ axis. The ratio of the yield on-axis versus off-axis (χ_{min}) is a measure of the crystalline perfection of the sample. The value of $\chi_{min}=0.04$ from the spectra shown in Fig. 3 is typical of values measured for transmission channeling samples which were very close to the χ_{min} measured in bulk silicon.[12] This shows that, for purposes of channeling, the thin crystals used in our transmission channeling studies were equivalent to high quality bulk silicon wafers.

^{4}He scattered near the beam exit side of the sample loses energy passing through Si and therefore reaches the detector with less energy than ^{4}He scattered near the beam-entry side of the sample. Thus the width of the RBS peak depends on the thickness of the silicon and the stopping power of ^{4}He in silicon.[20,21] The curve in Fig. 3 shows a computer simulation of the backscattering spectrum for a thin silicon target. From a fit to the back (i.e., low-energy) edge of the spectrum, the thickness of the sample was determined to be 0.36 ± 0.02 μm.

A second detector, which faced the beam-exit side of the sample and was in line with the analysis beam, analyzed D and H elastically recoiled from the sample by the ^{4}He beam. In order to detect recoiled D it is necessary to prevent scattered He from reaching the elastic recoil detector. This is done by placing a range foil in front of the detector, which is thick enough to stop the He but thin enough to transmit recoiled D and H ions. Aluminum foil 12 μm thick was used for the range foil. In addition, the central portion of the elastic recoil detector

must be covered by a blocking disk thick enough to stop all particles, to prevent H and D on the range foil from being recoiled into the detector. The detector configuration allowed particles recoiled from the sample through angles between 4.9° and 11.9° to enter the detector. Thus, the solid angle for elastic recoil detection (ERD) was 0.113 Sr.

Counts from recoiled H and D can be distinguished by their different energies, due to the factor of 2 mass difference and the kinematics of elastic scattering. ERD thus allows the areal densities of H and D on the sample to be independently measured. H was observed on samples with H-terminated surfaces prepared by rinsing in BOE. ERD showed that samples cleaned by the Shiraki method and dosed with atomic D as described above had only D with no detectable H. Furthermore the areal density (N) of H or D on the sample can be absolutely determined from the measured ERD yields which are given by

$$Y = n_{\mathrm{He}} N \Omega \sigma \ , \quad (1)$$

where n_{He} is the number of impinging He ions, Ω is the detector solid angle, and σ is the differential scattering cross sections for H or D recoiled by ^{4}He which are known.[22–24] Experimentally, n_{He} is determined by integrating the beam current used to make the measurement. The absolute accuracy of values for H and D coverage determined from ERD yields is estimated to be $\pm 10\%$ from the combined uncertainties in n_{He}, Ω, and σ. For comparisons between measured values, the relative accuracy is mainly determined by counting statistics.

The He analysis beam loses energy while passing through the silicon and therefore has a lower energy at the beam-exit surface than at the beam-entry surface. The resulting difference in energy between D recoiled from the beam-entry and beam-exit surfaces is not sufficient to distinguish counts from D on the beam-entry versus beam-exit surfaces from a single energy spectrum. However, the cross section for D recoiled by ^{4}He has a narrow resonance at 2.13 MeV,[24] whose width [68-keV full width at half maximum (FWHM)] is comparable to the energy lost by the ^{4}He analysis beam as it passes through the sample. This resonance allows the D coverage on the beam-entry and beam-exit surfaces to be independently determined by measuring the ERD yield as a function of analysis beam energy and then fitting the data to a D depth profile consisting of two δ functions. This method of resonance depth profiling has often been used with nuclear reactions which have narrow resonances.[25] Our fitting procedure used the ERD cross section measured by Bessesbacher, Stensgaard, and Vase[24] for a laboratory scattering angle of 10°. Furthermore we used a parametrization for the energy dependence of the cross section in the energy range between 2.0 and 2.3 MeV, consisting of a Lorentzian peak with a constant background.

Figure 4 shows a depth profile measurement of D on the transmission channeling sample. The filled circles show data taken with the analysis beam 1° away from the ⟨100⟩ axis after D on the beam-entry side had been partially removed by sputtering. The solid curves show the fit obtained using the Lorentzian parametrization for the

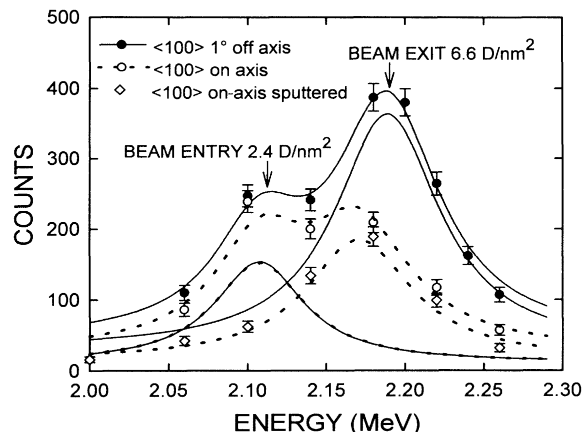

FIG. 4. ERD yield vs energy from D on the transmission channeling sample. The curves show fits to two Lorentzian peaks from D on the beam entry and beam exit surfaces. For the open symbols and dashed curves the analysis beam was aligned with the ⟨100⟩ axis. For the solid circles and solid curves the analysis beam was 1° away from the ⟨100⟩ axis.

ERD yield from D on the two surfaces. This measurement shows there is 6.6 D/nm^2 on the beam-exit surface and 2.4 D/nm^2 on the beam-entry surface. The measured D coverage on the beam-exit surface (6.6 D/nm^2) is equal (within the $\pm 10\%$ absolute accuracy of the measurement) to the number of Si atoms on the (100) surface which is 6.8 Si/nm^2. This fact, combined with the observation that doubling the exposure to atomic D did not significantly increase the D coverage, shows that the beam-exit surface was fully terminated by the monohydride.

The open circles in Fig. 4 shows a depth profile measurement taken with the analysis beam aligned along the ⟨100⟩ axis. The dashed curves show the corresponding fit. Compared to the data taken 1° off-axis, the yield from D on the beam-entry surface is the same but the yield from D on the beam-exit surface is smaller by a factor of 2. In addition, the peak from D on the beam-exit surface is shifted down in energy by about 10 keV. Both of these effects result from channeling. The reduced yield for the on-axis versus off-axis measurement results from a reduced ^{4}He flux at the hydrogen position under conditions of channeling along the ⟨100⟩ axis as discussed above. This is the effect we use to determine the D location. The energy shift results from the fact that under channeling conditions the ^{4}He flux is concentrated near the center of the channel where the electron density, and therefore the stopping power, is lower than average. The open diamonds in Fig. 4 show the ERD yield measured with the analysis beam aligned along the ⟨100⟩ axis, after further sputtering to remove all D from the beam-entry side of the sample. During the channeling measurement the D coverage remained constant, which shows that the analysis beam did not induce significant loss of D from the surface.

The channeling goniometer was designed to allow the

sample to be tilted up to 60° from normal to the beam without obstructing line of sight to the ERD or RBS detectors or the analysis beam. This permits measurements along the ⟨100⟩, ⟨110⟩, and ⟨111⟩ axes which require tilts of 0°, 45°, and 55° from normal incidence, respectively.

III. CHANNELING RESULTS

Channeling scans were measured at the ⟨100⟩, ⟨110⟩, and ⟨111⟩ axes on a sample prepared as described above to produce a saturated monohydride surface. The results are shown in Fig. 5. Since D on the beam-entry surface of this sample was removed by sputtering, the ERD yields shown in Fig. 5 are from D on the beam-exit surface only. The data shown in Figs. 3, 4, and 5 were all taken on the same sample. For each axis, ERD and RBS spectra were recorded at several angles between 0° and 1.2° from the axis. To average out planar channeling effects, the spectrum for each angle was the sum of measurements at 20 points around a circle of constant angle from the axis. The channeling data shown in Fig. 5 were taken with an analysis beam energy of 2 MeV. The beam energy at the exit surface is lower than 2 MeV due to energy lost while passing through the sample. This beam energy was chosen so that small variations in the beam energy at the exit surface due to channeling effects would not cause significant changes in the scattering cross section.

The main features of the channeling data shown in Fig. 5 can be qualitatively summarized as follows. On the ⟨100⟩ axis the ERD yield was lower by about a factor of 2 than the off-axis value. On the ⟨111⟩ axis the ERD yield was higher by about 25% compared to the off-axis value. On the ⟨110⟩ axis the ERD yield was about the same on-axis as off-axis but showed evidence of a small peak about 0.2° off-axis. Note that the factor of 2 reduction in ERD yield on the ⟨100⟩ axis is consistent with the decrease in ERD yield from D on the beam-exit surface due to channeling shown in Fig. 4 and discussed in Sec. II.

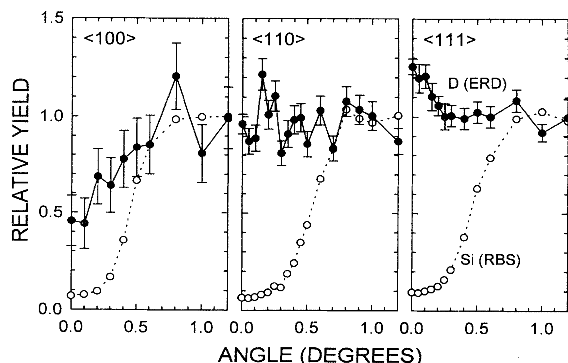

FIG. 5. Results from channeling scans. The filled circles show the ERD yield from D on the beam-exit surface, and the open circles show the RBS yield from the Si lattice.

IV. COMPUTER SIMULATIONS OF CHANNELING

Evaluation of the D location was done by comparing the measured channeling data (Fig. 5) with computer simulations of channeling. The simulations were done using a computer model developed by Bech Nielsen,[26] which is based on the continuum model for channeling and which includes dechanneling and vibrational motion of the D and Si atoms.

The Si(100) monohydride surface is known to reconstruct into symmetric dimer pairs by displacement of atoms forming the pair toward each other in the ⟨110⟩ direction from their lattice positions.[7,8] By symmetry the Si-D bonds should be in (110) planes normal to the surface which pass through the dimer pair. The geometry of the Si(100) monohydride surface is shown in Fig. 6. The dimer pairs may form in two orthogonal ⟨110⟩ directions on the (100) surface. The calculations assume equal numbers of dimers in the two directions.

Channeling scans for the ⟨100⟩, ⟨110⟩, and ⟨111⟩ axes were calculated for the grid of possible D locations relative to the Si lattice shown in Fig. 6. The best agreement between the measured and simulated channeling scans was obtained for D located at $x=0.05a$ and $z=0.25a$, where x and z are the displacement vectors parallel and perpendicular to the surface, respectively, to the D from the unreconstructed lattice site of the Si to which the D is bound, in units of the Si lattice constant $a=5.43$ Å. Figure 7 shows the simulated channeling scans for the ⟨100⟩, ⟨110⟩, and ⟨111⟩ axes for D locat-

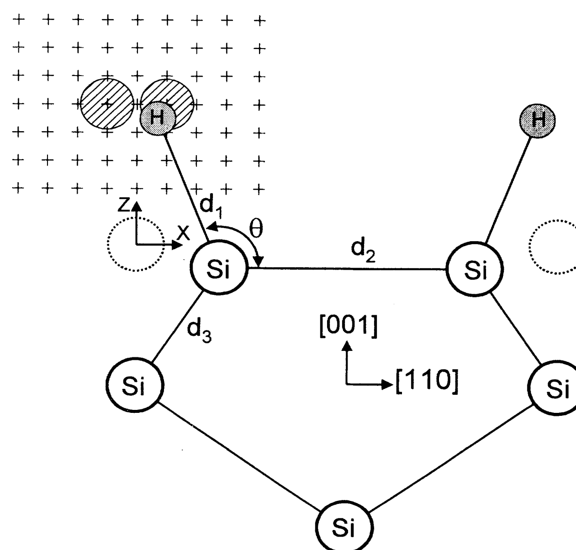

FIG. 6. The configuration of the Si(100) monohydride surface. The surface Si atoms are displaced from their original lattice sites (indicated by the dotted circles) toward each other to form dimer pairs. The array of crosses shows the grid on which channeling simulations were calculated. The crosshatched circles show the region within which the D must be located for agreement between simulated and measured channeling scans. The shaded circles labeled H show the H position predicted by *ab initio* calculations.

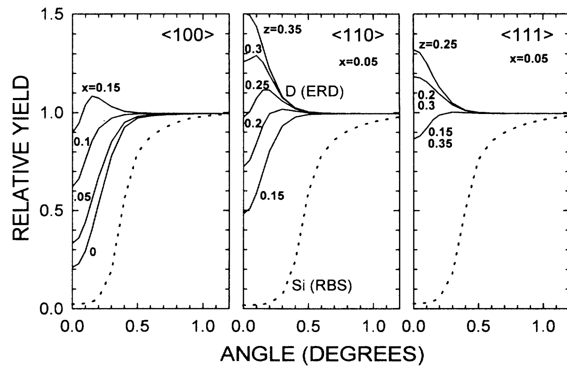

FIG. 7. Channeling scans calculated using Bech Nielsen's computer simulation. The dashed curves show the predicted RBS yield from Si. The solid curves show the ERD yield for D at the various locations indicated. The coordinates labeling the curves are given in units of the silicon lattice constant $a=5.43$ Å.

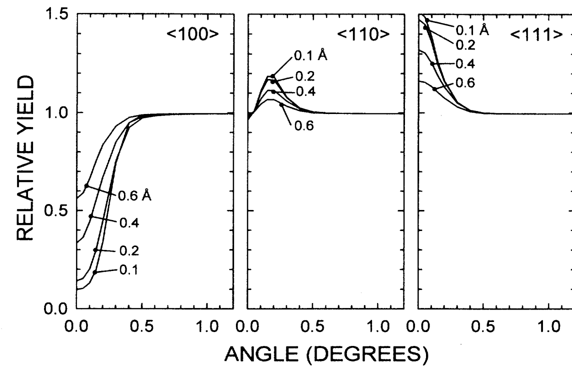

FIG. 8. Calculated channeling yield for various D vibrational amplitudes for D at $x=0.05a$ and $z=0.25a$. The labels for the curves indicate the two-dimensional rms vibrational amplitude.

ed at the best-fit position. Figure 7 also shows how the channeling scans are affected by changes in the D location. The $\langle 100 \rangle$ scan is not affected by displacements along the z direction, since this is along the direction of the analysis beam. Small changes in the x coordinate have a greater affect on the $\langle 100 \rangle$ scan than on the $\langle 110 \rangle$ and $\langle 111 \rangle$ scans. Thus the range of possible x coordinate values is most tightly constrained by the fit to the $\langle 100 \rangle$ scan and is estimated to be $0.05 \pm 0.04a$ or 0.3 ± 0.2 Å. The range of possible z coordinate values is most tightly constrained by the fit to the $\langle 110 \rangle$ scan, but the $\langle 111 \rangle$ scan gives almost the same range of possible z coordinate values which is estimated to be $0.25 \pm 0.04a$ or 1.36 ± 0.2 Å. The crosshatched circles in Fig. 6 show the regions within which the D must be located to give simulated channeling scans which agree with the measured channeling scans. The simulated channeling scans for D at a position (x,z) are the same as those for D at $(-x,z)$ because the two D atoms bound to a dimer pair are in symmetric positions with respect to the x coordinate.

Thermal motion of the D reduces the magnitude of the variations in scattering yield with angle as shown in Fig. 8. The agreement between calculated and measured (Fig. 5) channeling scans is best for a value of 0.4 Å for the two-dimensional rms vibrational amplitude of the D. This value is somewhat larger than the value of 0.2 Å obtained from a quantum harmonic-oscillator model using vibrational frequencies for Si-H measured by electron-energy-loss spectroscopy.[27] For a harmonic-oscillator model the vibrational frequencies for Si-D are lower than those of Si-H by a factor of 0.707 because of the mass difference, and most of the D motion at room temperature results from zero point motion of the Si-D bending mode. The two-dimensional (2D) rms vibrational amplitude of the Si was estimated to be 0.1 Å from the Si lattice Debye temperature.[28] The channeling scans shown in Fig. 7 used 2D rms vibrational amplitudes of 0.4 Å for D and 0.1 Å for Si.

The location of H on the Si(100) monohydride surface predicted by several *ab initio* calculations[1-6] are given in Table I. The positions of the H from the different calculations are in good agreement with each other. Averaging results from Refs. 1–6, we find that the *ab initio* calculations predict that (1) the bond length between the dimerized surface Si and the second-layer Si $d_3=2.35$ Å, which is equal to the Si-Si bond length of the bulk lattice; (2) the Si dimer spacing $d_2=2.42$ Å, (3) the Si-H bond length $d_1=1.51$ Å, which is close to the value of 1.48 Å for the Si-H bond length in the silane molecule; and (4) the angle between the Si dimer bond and the Si-H bond $\theta=110°$, which is very close to the tetrahedral bond angle of 109.5°. The average position of H from the six *ab initio* calculations is $x=0.185$ Å and $z=1.21$ Å. This calculated H position, indicated by the shaded circles labeled H in Fig. 6, lies within the crosshatched region, showing possible positions consistent with results from the channeling experiments. Thus the D location determined by channeling measurements agrees with the H position predicted by the *ab initio* calculations.

The location reported for H on the Si(100) monohydride surface from time-of-flight scattering and recoiling spectroscopy (TOF-SARS) experiment of Wang, Shi, and Rabalais[11] differs significantly from the location determined from our channeling experiments, and from the *ab initio* calculations (see Table I). In the TOF-SARS exper-

TABLE I. Geometry of H on the Si(100) monohydride surface. Parameters are defined in Fig. 7 and the text. References 1–6 are *ab initio* calculations. Reference 11 is a previously reported measurement by low-energy ion scattering.

d_1 (Å)	d_2 (Å)	d_3 (Å)	$\theta°$	x (Å)	z (Å)	Reference
1.47	2.35	2.35	109.5	0.26	1.16	1
1.53	2.37	2.33	110.2	0.21	1.17	2
1.51	2.47	2.35	109.4	0.18	1.24	3
1.55	2.40	2.34	109.0	0.22	1.24	4
1.51	2.43	2.36	114.7	0.08	1.19	5
1.48	2.51	2.38	110	0.16	1.27	6
1.22	2.97	2.35	133	−0.40	0.82	11
				0.27±0.2	1.36±0.2	this work

iments the H location was determined from measurements of the yield of H recoiled from the surface by 4-keV Ne^+ and Ar^+ ions at very small angles ($<4°$) of incidence to the surface. Their H position, given in Table I, was obtained from an analysis which used a shadow cone for single event scattering of Ne^+ and Ar^+ from Si and did not include multiple deflections of the incident ions. However as Wang, Shi, and Rabalais acknowledge, at the low ion energies and small angles of incidence used in their experiments, multiple deflections, i.e., surface channeling, are known to occur and are expected to have a significant effect on the trajectory of the analysis beam and hence on the location of the H obtained from analysis of the TOF-SARS data. Wang, Shi, and Rabalais acknowledge this difficulty and state that their value for the Si-H bond length is a lower limit.[11]

Our channeling experiments determine the location of the D relative to the bulk Si lattice. The length and direction of the surface Si-D bond also depend on the position of the surface Si atom to which the D is bound. The position of the surface Si obtained from averaging the six *ab initio* calculations listed in Table I is $x = 0.7$ Å and $z = -0.2$ Å. This position for the Si together with our position for the D gives values of $d_1 = 1.6 \pm 0.2$ Å and $\theta = 106 \pm 6°$ for the Si-D bond length and direction on the Si(100) monohydride surface.

ACKNOWLEDGMENTS

The author thanks Terry Guilinger for supplying the SIMOX wafers from which samples were fabricated, and Brian Bech Nielsen for furnishing the computer program used for the channeling simulations. This work was performed under the auspices of the U.S. Department of Energy and funded by its Office of Basic Energy Sciences, Division of Materials Science, under Contract No. DE-AC04-94AL85000.

[1]J. A. Appelbaum, G. A. Baraff, D. R. Hamann, H. D. Hagstrum, and T. Sakurai, Surf. Sci. **70**, 654 (1978).
[2]X. M. Zheng and P. V. Smith, Surf. Sci. **279**, 127 (1992).
[3]Z. Jing and J. L. Whitten, Phys. Rev. B **46**, 9544 (1992).
[4]J. E. Northrup, Phys. Rev. B **44**, 1419 (1991).
[5]C. J. Wu and E. A. Carter, Chem. Phys. Lett. **185**, 172 (1991).
[6]Y. J. Chabal and K. Raghavachari, Phys. Rev. Lett. **53**, 282 (1984).
[7]J. J. Boland, Surf. Sci. **261**, 17 (1992).
[8]J. J. Boland, Adv. Phys. **42**, 129 (1993).
[9]T. Sakurai and H. D. Hagstrum, Phys. Rev. B **14**, 1593 (1976).
[10]K. Oura, J. Yamane, K. Umezawa, M. Naitoh, F. Shoji, and T. Hanawa, Phys. Rev. B **41**, 1200 (1990).
[11]Y. Wang, M. Shi, and J. W. Rabalais, Phys. Rev. B **48**, 1678 (1993).
[12]L. C. Feldman, J. W. Mayer, and S. T. Picraux, *Materials Analysis by Ion Channeling* (Academic, New York, 1982).
[13]I. Stensgaard and F. Jakobsen, Phys. Rev. Lett. **54**, 711 (1985).
[14]K. Mortensen, F. Besenbacher, I. Stensgaard, and W. R. Wampler, Surf. Sci. **205**, 433 (1988).
[15]F. Besenbacher, I. Stensgaard, and K. Mortensen, Surf. Sci. **191**, 288 (1987).
[16]N. W. Cheung and J. W. Mayer, Phys. Rev. Lett. **46**, 671 (1981).
[17]L. E. Seiberling, P. F. Lyman, and M. W. Grant, J. Vac. Sci. Technol. A **11**, 715 (1993).
[18]Hughes Danbury Optical Systems, Inc., 100 Wooster Heights Road, Danbury, CT 06810.
[19]A. Ishizaka and Y. Shiraki, J. Electrochem. Soc. **133**, 666 (1986).
[20]W. K. Chu, J. W. Mayer, and M. A. Nicolet, *Backscattering Spectrometry* (Academic, New York, 1978).
[21]J. F. Ziegler, *Helium Stopping Powers and Ranges in All Elemental Matter* (Pergamon, New York, 1977).
[22]E. Szilagyi, F. Paszti, A. Manuaba, C. Hajdu, and E. Kotai, Nucl. Instrum. Methods B **43**, 502 (1989).
[23]J. E. E. Baglin, A. J. Kellock, M. A. Crockett, and A. H. Smith, Nucl. Instrum. Methods B **64**, 469 (1992).
[24]F. Besenbacher, I. Stensgaard, and P. Vase, Nucl. Instrum. Methods B **15**, 459 (1986).
[25]J. F. Ziegler *et al.*, Nucl. Instrum. Methods **149**, 19 (1978).
[26]B. Bech Nielsen, Phys. Rev. B **37**, 6353 (1988).
[27]P. Dumas and Y. J. Chabal, J. Vac. Sci. Technol. A **10**, 2160 (1992).
[28]D. S. Gemmel, Rev. Mod. Phys. **46**, 129 (1974).

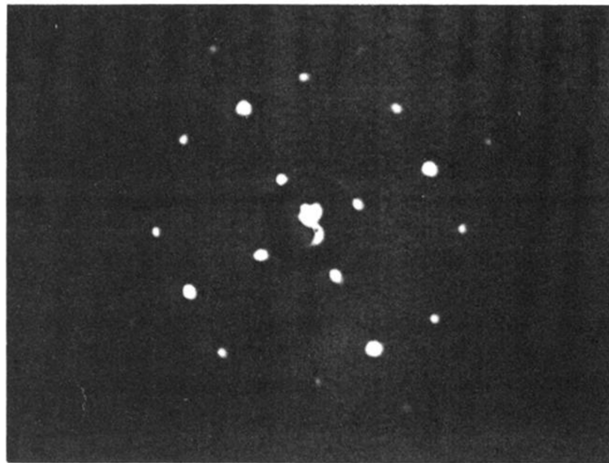

FIG. 2. LEED image showing the 2×1 surface structure taken with an electron energy of 55 eV after dosing the sample with D.